Int. J. Solids Structures Vol. 29, No. 20, pp. 2503–2525, 1992
Printed in Great Britain.

0020–7683/92 $5.00 + .00

SHAPE DESIGN SENSITIVITY ANALYSIS FOR GEOMETRICALLY AND MATERIALLY NONLINEAR PROBLEMS BY THE BOUNDARY ELEMENT METHOD

Q. ZHANG
Mechanical Engineering Department, Westhollow Research Center, Shell Development Company, P.O. Box 1380, Houston, TX 77251, U.S.A.

S. MUKHERJEE
Department of Theoretical and Applied Mechanics, Cornell University, Ithaca, NY 14853, U.S.A.

and

A. CHANDRA
Department of Aerospace and Mechanical Engineering, The University of Arizona, Tucson, AZ 85721, U.S.A.

(*Received* 2 *September* 1991; *in revised form* 1 *February* 1992)

Abstract—This paper is concerned with the determination of design sensitivity coefficients (DSCs) for "fully nonlinear" problems—i.e. problems with both material and geometric nonlinearities—in solid mechanics. The elastic strains are assumed to be small, but the nonelastic (plastic or visco-plastic) strains, as well as rotations, can be arbitrarily large. DSCs here refer to rates of change of response variables, such as displacements or stresses, in a deforming solid body, with respect to parameters (called design variables) that define the initial (undeformed) shape of the body. These DSCs are history dependent.

The direct differentiation approach (DDA) of the relevant derivative boundary element method (DBEM) formulation is employed to obtain the DSCs. A general computer program is developed for the analysis of two-dimensional (plane strain and plane stress) problems. Numerical results are obtained for illustrative problems and are compared against direct solutions. The results from the two methods agree almost perfectly for these problems.

This research has potential applications in the optimization of manufacturing processes such as extrusion, rolling or forging.

INTRODUCTION

The subject of this paper is the calculation of design sensitivity coefficients (DSCs) for "fully nonlinear" solid mechanics problems by the boundary element method (BEM). A "fully nonlinear" problem is defined as one that includes both material (elasto–plastic or elasto–viscoplastic) and geometrical (large strains and rotations) nonlinearities. Problems of interest are those with small elastic strains but with large inelastic strains and rotations. Such problems have important applications in metal forming.

DSCs are rates of change of response quantities such as stress or displacement in a loaded body with respect to design variables. These design variables could be shape parameters that control the (initial) shape of part or all of the boundary of a body, or they could be boundary conditions, material parameters, etc. Shape parameters as design variables are of concern in this work.

DSCs are useful in diverse problems. An example is a design problem where the performance of a modified design can be obtained from that of an initial design by using a Taylor series expansion about the initial design. They are useful in solving inverse problems (Zabaras *et al.*, 1988) and reliability analyses (Ang and Tang, 1975). A very important area for the application of DSCs with respect to shape parameters is in optimal shape design. An optimization process starts with a preliminary design and calculation of DSCs for this design. Such a nonlinear programming algorithm [e.g. Vanderplaats (1983)] uses the preliminary design and its sensitivities to propose a new design. The goal is to optimize an objective function without violating the constraints (typically allowable stresses or

displacements) of a problem. This process is carried out in an iterative manner, producing a succession of designs, until an optimal design is obtained.

There is a rich literature on the subject of determination of DSCs for linear problems in mechanics, such as elasticity or heat transfer [see, for example, Haug *et al.* (1986)]. Basically, three different approaches have been used—the finite difference approach (FDA), the adjoint structure approach (ASA) and the direct differentiation approach (DDA). Also, both the finite element method (FEM) and the boundary element method (BEM) have been used for these analyses by different researchers.

Attention is now focused on a very promising approach—DDA of the governing boundary integral equations of a problem. Here, the exact differentiation eliminates errors that might occur from the use of finite differencing and leads to closed-form integral equations of the desired sensitivities. These equations are then solved by numerical discretization. This approach is very accurate and efficient.

Recently, a number of researchers have published papers on the determination of DSCs for linear elastic problems by the BEM. These include planar (Barone and Yang, 1988; Kane and Saigal, 1988; Choi and Choi, 1990; Zhang and Mukherjee, 1991a), axisymmetric (Saigal *et al.*, 1989; Rice and Mukherjee, 1990), and three-dimensional (Barone and Yang, 1989; Aithal *et al.*, 1991) problems. Work on second order DSCs for linear elasticity problems has just been published by Zhang and Mukherjee (1991b).

The problem of DSCs for nonlinear solid mechanics problems has only recently begun to attract attention. Arora and his co-workers (Wu and Arora, 1987; Cardoso and Arora, 1988; Tsay and Arora, 1990; Tsay *et al.*, 1990), Choi and his co-workers (Choi and Santos, 1987; Santos and Choi, 1988; Park and Choi, 1990) and Tortorelli (1988, 1990) have attempted nonlinear sensitivity problems with the FEM. Mukherjee and Chandra (1989) have presented a BEM formulation for shape sensitivities for small-strain elasto–plastic and elasto–viscoplastic problems, and Zhang *et al.* (1992) have recently obtained numerical results for this class of problems. A BEM formulation for fully nonlinear problems involving both material and geometric nonlinearities has just been published by Mukherjee and Chandra (1991). Many new and interesting issues, of a theoretical as well as numerical nature, have arisen during the numerical realization of this class of problems. These issues are discussed in the present paper.

Inclusion of materially and geometrically nonlinear effects opens new doors in DSCs and optimization research in that optimization of processes, rather than just products, can now be attempted. One can, for example, attempt to optimize the shape of a die for extrusion or the shape of a pre-form for forging. These problems, however, become quite complicated, since nonlinearities are involved. Accordingly, the response variables, and therefore their sensitivities, become history dependent. Also, since nonelastic strain rates are typically strongly nonlinear and sensitive functions of stresses, and DSCs are derivatives of history-dependent response variables, the numerical process must be extremely accurate in order to deliver meaningful results for the desired DSCs. In fact, in order to obtain the elasto–viscoplastic results presented by Zhang *et al.* (1992), even a half percent numerical error in some integrals of logarithmically singular functions proved to be intolerable and the integration algorithm had to be improved even further. The BEM, on the other hand, is known to be extremely accurate if it is implemented with care. Thus, the DDA of the BEM has very strong potential for success in solving these complicated problems with sufficient accuracy.

This paper begins with a derivative boundary element method (DBEM) formulation for fully nonlinear problems in solid mechanics. A BEM formulation for this class of problems was first presented by Chandra and Mukherjee (1983) [see also Mukherjee and Chandra (1987)]. An updated Lagrangian approach was used in that work. The present work on sensitivities requires analytical differentiation of the BEM equations with respect to geometrical parameters that define the initial (undeformed) shape of a body. An updated Lagrangian formulation of the deformation problem (Mukherjee and Chandra, 1987) may specialize the governing equations too soon and lead to errors in the sensitivity equations that are obtained by differentiation of these equations. Therefore, the formulation of Mukherjee and Chandra (1987) is revisited in this paper. The governing integral equations

for the deformation problem are now derived in the current configuration of a body without the simplifications that arise out of the use of an updated Lagrangian formulation. This discussion is followed by a presentation of the DBEM equations on the boundary and inside a body.

It is also important to mention the salient features of the DBEM formulation. This formulation, presented by Ghosh *et al.* (1986) and Ghosh and Mukherjee (1987), uses tractions and displacement derivatives (rather than tractions and displacements) as primary variables on the boundary of a body. This idea has two significant advantages over the standard BEM. The first is that the kernels are only logarithmically singular for two-dimensional elasticity problems. These weakly singular kernels can be integrated very accurately by log-weighted Gaussian integration. Extremely accurate integration of singular functions is an essential requirement for accurate determination of sensitivities. The second advantage is that boundary stresses can be obtained from the boundary values of tractions and displacement derivatives by purely algebraic calculations. This allows one to determine stresses and their sensitivities, on the boundary of a body, with excellent accuracy.

The BEM formulation for the deformation problem is followed by the sensitivity formulation for planar problems. Interesting issues arise here, such as the differentiation of a boundary length element or a normal vector in the current configuration, with respect to shape variables that are only defined in the undeformed configuration. Also, the kernels of the integral equations must be differentiated with respect to shape variables that define the initial (undeformed) configuration of the body.

Following a brief discussion of the modeling of corners in a body [further detailed discussions are given by Zhang and Mukherjee (1991a) and Zhang *et al.* (1992)], a section on the numerical implementation of the deformation and the sensitivity formulation is presented. The solution proceeds by marching forward in time, together with the updating of the shape of the deforming body as required. Iterations are necessary within each time step. An updated Lagrangian formulation is *not* considered appropriate here and is not used in this paper.

The last substantial section of this paper is concerned with illustrative one-dimensional problems—homogeneous large deformation of a body in plane strain or in plane stress. Some general formulae, derived earlier in the paper, are analytically validated for these one-dimensional problems. This is followed by the presentation of numerical results for one-dimensional planar problems. A general two-dimensional computer program, based on the DBEM formulation discussed above, is used to generate these numerical results. These results are checked against "direct" solutions, which are considered to be nearly as accurate as the exact solutions of these one-dimensional problems. Detailed considerations of these one-dimensional problems serve as essential checks of the computer algorithm for two-dimensional problems. It is felt that obtaining numerical results from a complicated computer program, such as the one discussed in this paper, is meaningless without careful validation of the numerical results in simple situations.

DERIVATIVE BOUNDARY ELEMENT FORMULATION

Integral equations in the current configuration

As discussed above, the boundary integral equations for fully nonlinear problems are derived here without making the assumptions associated with an updated Lagrangian formulation. Such a formulation had been employed in previous work (Mukherjee and Chandra, 1987). The equations in this section are valid for three-dimensional problems so, unless otherwise indicated, the range of indices is 1, 2, 3.

Kinematic and constitutive assumptions. Referring to a set of spatially fixed rectangular Cartesian co-ordinates, a material particle in a body is assumed to have co-ordinates $\mathbf{X}$ in the original undeformed configuration (at time zero) and $\mathbf{x}$ in the current configuration (at time t). The usual definitions are adopted for the deformation gradient $\mathbf{F}$, the velocity gradient $\mathbf{h}$ and its symmetric and antisymmetric parts. Thus,

$$\mathbf{F} = \frac{\partial \mathbf{x}}{\partial \mathbf{X}}, \qquad \mathbf{h} = \nabla \mathbf{v}, \qquad \mathbf{d} = \tfrac{1}{2}(\mathbf{h}+\mathbf{h}^{\mathrm{T}}), \qquad \boldsymbol{\omega} = \tfrac{1}{2}(\mathbf{h}-\mathbf{h}^{\mathrm{T}}), \tag{1–4}$$

where $\mathbf{v}$ is the velocity vector and ∇ is the gradient operator in the current configuration (i.e. $h_{ij} = \partial v_i/\partial x_j$).

The key constitutive assumptions, which are valid in the current configuration, are as follows: the first assumption is that the tensor $\mathbf{d}$ can be additively decomposed into an elastic and a nonelastic part:

$$\mathbf{d} = \mathbf{d}^{(e)} + \mathbf{d}^{(n)}. \tag{5}$$

The second is that the material is homogeneous and isotropic, and the elastic field obeys the hypoelastic relationship (Fung, 1965)

$$\hat{\boldsymbol{\sigma}} = \lambda \operatorname{tr}(\mathbf{d}^{(e)})\mathbf{I} + 2G\mathbf{d}^{(e)}, \tag{6}$$

where $\boldsymbol{\sigma}$ is the Cauchy stress, λ and G are Lamé constants, tr denotes the trace of a tensor, and $\mathbf{I}$ is the identity tensor. A hat ($\hat{}$) over $\boldsymbol{\sigma}$ denotes one of its objective rates. The Jaumann rate is adopted here, but other objective rates can be used if desired. [See, for example, Chandra and Mukherjee (1986) for the choice of objective rates in the presence of large shearing strains.] Thus,

$$\hat{\boldsymbol{\sigma}} = \dot{\boldsymbol{\sigma}} + \boldsymbol{\sigma}\cdot\boldsymbol{\omega} - \boldsymbol{\omega}\cdot\boldsymbol{\sigma} \tag{7}$$

in terms of the material rate of the Cauchy stress (denoted here as $\dot{\boldsymbol{\sigma}}$).

A general form of a nonelastic constitutive law governing the behavior of $\mathbf{d}^{(n)}$ is

$$\mathbf{d}^{(n)} = \mathbf{f}(\boldsymbol{\sigma}, \mathbf{q}_1, \mathbf{q}_2, \ldots, \mathbf{q}_k) \quad \text{and} \quad \hat{\mathbf{q}}_p = \mathbf{g}_p(\boldsymbol{\sigma}, \mathbf{q}_1, \mathbf{q}_2, \ldots, \mathbf{q}_k), \tag{8, 9}$$

where $\mathbf{q}_p$, $p = 1, 2, \ldots, k$ (where k is usually a small integer), are suitably defined state variables, which can be scalars or tensors. A general discussion of such unified viscoplastic constitutive models, using state variables, can be found in Mukherjee (1982). A conventional plasticity model for material behavior can also be employed if desired. Discussion of the choice of a specific constitutive model is deferred until later in this paper.

Relationships between stress rates. The relationships between the Cauchy stress $\boldsymbol{\sigma}$, the Kirchhoff stress $\boldsymbol{\tau}$ and the Lagrange (nominal, nonsymmetric) stress S are

$$\boldsymbol{\tau} = J\boldsymbol{\sigma}, \qquad \mathbf{S} = \mathbf{F}^{-1}\cdot\boldsymbol{\tau}, \tag{10, 11}$$

where $J = \det(\mathbf{F})$.

It is easy to prove the following relationships:

$$\dot{J} = J \operatorname{tr}(\mathbf{d}), \qquad \mathbf{d} + \boldsymbol{\omega} = \dot{\mathbf{F}}\cdot\mathbf{F}^{-1}. \tag{12, 13}$$

Using eqns (7) and (10)–(13), some straightforward algebraic manipulations reveal the relationship

$$\hat{\boldsymbol{\sigma}} = \frac{\mathbf{F}\cdot\dot{\mathbf{S}}}{J} + \mathbf{g}, \quad \text{where} \quad \mathbf{g} = \boldsymbol{\sigma}\cdot\boldsymbol{\omega} + \mathbf{d}\cdot\boldsymbol{\sigma} - (\operatorname{tr}\mathbf{d})\boldsymbol{\sigma}. \tag{14, 15}$$

Also, in the current configuration,

$$\tau^{(c)} = \mathbf{n}\cdot\hat{\boldsymbol{\sigma}} \quad \text{and} \quad \tau^{(L)} = \tau^{(c)} - \mathbf{n}\cdot\mathbf{g} = \mathbf{n}\cdot\frac{\mathbf{F}\cdot\dot{\mathbf{S}}}{J}, \tag{16, 17}$$

where $\tau^{(c)}$ and $\tau^{(L)}$ are the Cauchy and Lagrange traction rates, respectively, and $\mathbf{n}$ is the unit outward normal to a body at a point on its boundary.

Betti's theorem. The starting point of the BEM formulation is Betti's reciprocal theorem. In the current configuration (Mukherjee and Chandra, 1987),

$$\int_B \hat{\boldsymbol{\sigma}} : \boldsymbol{\varepsilon}^{(R)}\, dv = \int_B \boldsymbol{\sigma}^{(R)} : \mathbf{d}^{(c)}\, dv, \quad \text{where} \quad \boldsymbol{\sigma}^{(R)} = \lambda\, \mathrm{tr}\,(\boldsymbol{\varepsilon}^{(R)})\mathbf{I} + 2G\boldsymbol{\varepsilon}^{(R)} \tag{18, 19}$$

and $\mathbf{a} : \mathbf{b} = a_{ij}b_{ij}$ for any two second rank tensors $\mathbf{a}$ and $\mathbf{b}$. The variables with superscript R are the reference field variables due to a point force in an infinite, linear elastic, isotropic solid undergoing infinitesimal deformations. They satisfy the usual field equations of linear elasticity. Also,

$$u_i^{(R)} = U_{ij}e_j, \qquad \tau_i^{(R)} = T_{ij}e_j, \tag{20, 21}$$

where $\mathbf{u}^{(R)}$ and $\tau^{(R)}$ are the displacements and boundary tractions for linear elasticity and U_{ij} and T_{ij} are the usual Kelvin kernels [see, for example, Mukherjee (1982)]. Finally, e_i are Cartesian unit base vectors.

Using the definition of $\boldsymbol{\varepsilon}^{(R)}$ in terms of $\mathbf{u}^{(R)}$, together with eqns (14) and (20), the left-hand side of eqn (18) becomes

$$\int_B \hat{\boldsymbol{\sigma}} : \boldsymbol{\varepsilon}^{(R)}\, dv = e_k \int_B \left(\frac{\mathbf{F}\cdot\dot{\mathbf{S}}}{J}\right)_{ij} U_{jk,i}\, dv + e_k \int_B U_{jk,i} g_{ij}\, dv. \tag{22}$$

Using the divergence theorem, together with eqns (14), (16) and (17), one gets

$$e_k \int_B \frac{F_{im}\dot{S}_{mj}}{J} U_{jk,i}\, dv = e_k \int_{\partial B} U_{jk}\tau_j^{(L)}\, ds - e_k \int_B \left(\frac{F_{im}\dot{S}_{mj}}{J}\right)_{,i} U_{jk}\, dv, \tag{23}$$

where ∂B is the boundary of the domain B.

The second term on the right-hand side of eqn (23) can be shown to vanish as a consequence of the rate of equilibrium equation (in the undeformed configuration) and Nanson's formula (see the Appendix). Consequently,

$$\int_B \hat{\boldsymbol{\sigma}} : \boldsymbol{\varepsilon}^{(R)}\, dv = e_j \int_{\partial B} U_{ij}\tau_i^{(L)}\, ds + e_j \int_B U_{ij,m} g_{mi}\, dv. \tag{24}$$

The treatment of the right-hand side of Betti's theorem, eqn (18), follows the same approach as that given in detail by Mukherjee and Chandra (1987). The result is

$$\int_B \boldsymbol{\sigma}^{(R)} : \mathbf{d}^{(c)}\, dv = e_j \int_{\partial B} T_{ij}v_i\, ds + e_j \int_B \Delta(p, q)\delta_{ij}v_i\, dv - e_j \int_B 2GU_{ij,k}\, \mathrm{d}_{ik}^{(n)}\, dv, \tag{25}$$

where Δ is the Dirac delta function, δ_{ij} is the Kronecker delta, and p and q are source and field points, respectively, inside the body. In the above, it is assumed that $\mathrm{d}_{kk}^{(n)} = 0$.

Finally, the following integral relationship is obtained in the current configuration:

$$v_j(p) = \int_{\partial B} [U_{ij}(p, Q)\tau_i^{(L)}(Q) - T_{ij}(p, Q)v_i(Q)]\, ds(Q) + \int_B 2GU_{ij,k}(p, q)\, d_{ik}^{(n)}(q)\, dv(q) + \int_B U_{ij,m}(p, q)g_{mi}(q)\, dv(q), \quad (26)$$

where P and Q are source and field points, respectively, on the boundary ∂B of the body.

It is interesting to note that the above equation is almost the same as eqn (3.36) in Mukherjee and Chandra (1987) where the updated Lagrangian formulation was employed. The only difference is eqn (17) for $\tau^{(L)}$ in the current configuration. Please see the Appendix for further discussion of this issue.

DBEM equations for plane strain problems

The derivative boundary element formulation, as mentioned before, uses derivatives of displacements (or velocities) together with tractions (or traction rates) as primary boundary variables. For two-dimensional problems, partial integration is carried out on the term $T_{ij}v_i$ in eqn (26) so that one gets $\delta_i = \partial v_i/\partial s$ (where s is the distance measured along ∂B) as the boundary variable, together with a kernel W_{ij}. When the distance between a source and a field point (denoted by r) tends to zero, this kernel has a singularity of the order of $\ln r$. This is weaker compared to the $1/r$ singularity of T_{ij}. Details are given by Ghosh *et al.* (1986). Unless otherwise indicated, the range of indices in this section is 1, 2.

Boundary equations. The boundary integral equation corresponding to eqn (26), with $p \to P$, has the form

$$0 = \int_{\partial B} [U_{ij}(\mathbf{b}, P, Q)\tau_i^{(L)}(\mathbf{b}, Q) - W_{ij}(\mathbf{b}, P, Q)\delta_i(\mathbf{b}, Q)]\, ds(\mathbf{b}, Q) + \int_B [2GU_{ij,k}(\mathbf{b}, P, q)\, d_{ik}^{(n)}(\mathbf{b}, q)]\, da(\mathbf{b}, q) + \int_B U_{ij,m}(\mathbf{b}, P, q)g_{mi}(\mathbf{b}, q)\, da(\mathbf{b}, q). \quad (27)$$

Here, $k \equiv \partial/\partial x_k(q)$. The components of the vector $\mathbf{b}$ are shape design variables that define the initial (undeformed) shape of the body. The dependence of quantities on $\mathbf{b}$ are noted above in explicit form since eqn (27) will be differentiated later with respect to design variables. The kernel U_{ij} is given in many references [e.g. Mukherjee (1982)], and the explicit form of W_{ij} is given by Ghosh *et al.* (1986). They are both $\ln r$ singular.

It should be noted that for some problems with prescribed velocity on a portion ∂B_1 of ∂B, prescription of δ on ∂B_1 may lead to loss of information on the velocity itself. This may lead to loss of uniqueness of the solution obtained from this formulation. In such cases, this difficulty can be overcome by appending constraint equations of the type

$$\int_A^B \delta\, ds = \mathbf{v}(B) - \mathbf{v}(A), \quad (28)$$

where A and B are suitably chosen points on the boundary ∂B.

Stress rates and spin on the boundary. A boundary algorithm is very convenient to determine stress rates and spin, at a regular boundary point, in terms of the primary variables $\tau^{(L)}$ (or $\tau^{(c)}$) and δ, together with $\mathbf{d}^{(n)}$. In order to do this, one can use the algebraic boundary equations given by Mukherjee and Chandra (1991). [See Sladek and Sladek (1986) and Cruse and Vanburen (1971) for the linear elastic case.] These equations [from Mukherjee and Chandra (1991)] can, however, be solved explicitly, to obtain the stress rates and spins on the boundary:

$$\dot{\sigma}_{ij} = A_{ijk}\tau_k^{(c)} + B_{ijk}\delta_k + C_{ijkl}d_{kl}^{(n)} + D_{ij}\,\mathrm{d}_{kk}^{(n)}, \qquad h_{ij} = E_{ijk}\tau_k^{(c)} + F_{ijk}\delta_k + G_{ijkl}\,\mathrm{d}_{kl}^{(n)}, \tag{29, 30}$$

where

$$A_{ijk} = (n_i n_j + c_1 t_i t_j)n_k + (n_i t_j + n_j t_i)t_k,$$
$$B_{ijk} = c_2 t_i t_j t_k,$$
$$C_{ijkl} = -c_2 t_i t_j t_k t_l,$$
$$D_{ij} = \nu c_2 t_i t_j,$$
$$E_{ijk} = \frac{c_3}{2G} n_i n_j n_k + \frac{1}{G} t_i n_j t_k,$$
$$F_{ijk} = \gamma_{ij} n_k + t_i t_j t_k - c_1 n_i n_j t_k,$$
$$G_{ijkl} = c_3 n_i n_j n_k n_l + 2t_i n_j n_k t_l,$$

with $c_1 = \nu/(1-\nu)$, $c_2 = 2G/(1-\nu)$, $c_3 = (1-2\nu)/(1-\nu)$, ν is the Poisson's ratio of the material, and t_i are the components of the unit (anticlockwise) tangent vector to ∂B at a point on it. Finally, $\gamma_{11} = \gamma_{22} = 0$ and $\gamma_{12} = -\gamma_{21} = 1$.

The spin can be obtained from h_{ij} by using eqn (4) and the material rate of σ can be obtained from its Jaumann rate from eqn (7).

Internal equations. Velocity gradients and stress rates are also required at points inside the body. To this end, the version of eqn (27) at an internal point is first differentiated at a source point $x(p)$. As discussed by Mukherjee and Chandra (1991), this procedure leads to differentiation of an integral whose kernel is already $1/r$ singular. This problem can be avoided by using the method proposed by Huang and Du (1988). The final equation can be expressed as

$$\begin{aligned} h_{jI}(\mathbf{b}, p) = &\int_{\partial B} [U_{ij,I}(\mathbf{b}, p, Q)\tau_i^{(L)}(\mathbf{b}, Q) - W_{ij,I}(\mathbf{b}, p, Q)\delta_i(\mathbf{b}, Q)]\,\mathrm{d}s(\mathbf{b}, Q) \\ &- 2G d_{ik}^{(n)}(\mathbf{b}, p)\int_{\partial B} U_{ij,k}(\mathbf{b}, p, Q)n_l(\mathbf{b}, Q)\,\mathrm{d}s(\mathbf{b}, Q) \\ &- g_{mi}(\mathbf{b}, p)\int_{\partial B} U_{ij,m}(\mathbf{b}, p, Q)n_l(\mathbf{b}, Q)\,\mathrm{d}s(\mathbf{b}, Q) \\ &+ \int_B 2G U_{ij,kI}(\mathbf{b}, p, q)[\mathrm{d}_{ik}^{(n)}(\mathbf{b}, q) - d_{ik}^{(n)}(\mathbf{b}, p)]\,\mathrm{d}a(\mathbf{b}, q) \\ &+ \int_B U_{ij,mI}(\mathbf{b}, p, q)[g_{mi}(\mathbf{b}, q) - g_{mi}(\mathbf{b}, p)]\,\mathrm{d}a(\mathbf{b}, q), \end{aligned} \tag{31}$$

where

$$,I \equiv \frac{\partial}{\partial x_I(p)} \quad \text{and} \quad h_{jI} = \frac{\partial v_j}{\partial x_I(p)}.$$

Since

$$d_{ik}^{(n)}(\mathbf{b}, q) - d_{ik}^{(n)}(\mathbf{b}, p) \sim \mathrm{O}(r) \quad \text{and} \quad g_{mi}(\mathbf{b}, q) - g_{mi}(\mathbf{b}, p) \sim \mathrm{O}(r)$$

the domain integrals are now only $1/r$ singular. Rajiyah and Mukherjee (1987) also present alternate ways of treating these differentiated domain integrals.

Stress rates at an internal point. The hypoelastic law [eqn (6)] can be used to obtain the Jaumann rate of $\boldsymbol{\sigma}$ at an internal point from $\mathbf{h}$ and $\mathbf{d}^{(n)}$. It is convenient to rewrite this equation as

$$\hat{\sigma}_{ij} = \lambda h_{kk}\delta_{ij} + G(h_{ij} + h_{ji}) - 2Gd_{ij}^{(n)}. \tag{32}$$

Finally, the material rate of the Cauchy stress is obtained from the Jaumann rate from eqn (7). The corresponding equations for plane stress are given in Zhang (1991) and are not repeated here in the interest of brevity.

SENSITIVITY FORMULATION FOR PLANE STRAIN

Sensitivity equations, based on the direct analytical differentiation of the relevant DBEM equations, are given in this section. Shape perturbations of only the undeformed initial configuration **X** are considered in this work (Fig. 1), so that the shape design vector $\mathbf{b}$ is only defined in this configuration. The plane stress sensitivity equations are analogous to these equations. Unless otherwise indicated, the range of indices in this section is 1, 2.

Boundary equations

The first step is the differentiation of eqn (27) with respect to a (scalar) design variable b, which is a component of the vector $\mathbf{b}$. Let a superscribed $^{\bullet}$ denote the design derivative (w.r.t. b) of a variable of interest, and a superscribed $^{\circ}$ and $^{\hat{}}$ denote design derivatives of its material rate and of its Jaumann rate, respectively, in the configuration **X** (i.e. $\dot{\sigma}_{ij} = \mathrm{d}\sigma_{ij}/\mathrm{d}b$, $\dot{\delta}_{ij} = \mathrm{d}\dot{\sigma}_{ij}/\mathrm{d}b$, $\hat{\dot{\sigma}}_{ij} = \mathrm{d}\hat{\sigma}_{ij}/\mathrm{d}b$). Now, one obtains the equation

$$\begin{aligned}
0 = &\int_{\partial B} [U_{ij}(\mathbf{b}, P, Q)\dot{\tau}_i^{(L)}(\mathbf{b}, Q) - W_{ij}(\mathbf{b}, P, Q)\dot{\delta}_i(\mathbf{b}, Q)]\,\mathrm{d}s(\mathbf{b}, Q) \\
&+ \int_{\partial B} [\dot{U}_{ij}(\mathbf{b}, P, Q)\tau_i^{(L)}(\mathbf{b}, Q) - \dot{W}_{ij}(\mathbf{b}, P, Q)\delta_i(\mathbf{b}, Q)]\,\mathrm{d}s(\mathbf{b}, Q) \\
&+ \int_{\partial B} [U_{ij}(\mathbf{b}, P, Q)\tau_i^{(L)}(\mathbf{b}, Q) - W_{ij}(\mathbf{b}, P, Q)\delta_i(\mathbf{b}, Q)]\,\mathrm{d}\dot{s}(\mathbf{b}, Q) \\
&+ \int_B [2GV_{ijk}(\mathbf{b}, P, q)\,\dot{\mathrm{d}}_{ik}^{(n)}(\mathbf{b}, q)]\,\mathrm{d}a(\mathbf{b}, q) + \int_B [2G\dot{V}_{ijk}(\mathbf{b}, P, q)\,\mathrm{d}_{ik}^{(n)}(\mathbf{b}, q)]\,\mathrm{d}a(\mathbf{b}, q) \\
&+ \int_B [2GV_{ijk}(\mathbf{b}, P, q)\,\mathrm{d}_{ik}^{(n)}(\mathbf{b}, q)]\,\mathrm{d}\dot{a}(\mathbf{b}, q) + \int_B V_{ijm}(\mathbf{b}, P, q)\dot{g}_{mi}(\mathbf{b}, q)\,\mathrm{d}a(\mathbf{b}, q)
\end{aligned}$$

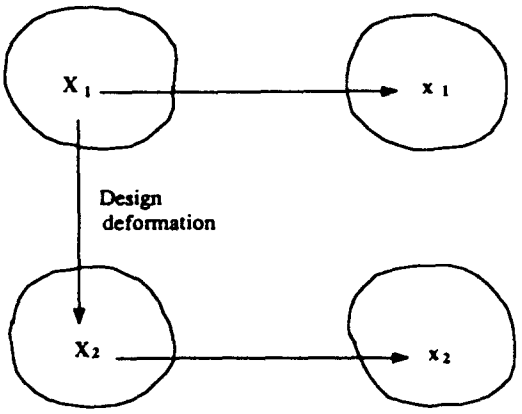

Fig. 1.

$$+\int_B \dot{V}_{ijm}(\mathbf{b}, P, q) g_{mi}(\mathbf{b}, q)\, \mathrm{d}a(\mathbf{b}, q) + \int_B V_{ijm}(\mathbf{b}, P, q) g_{mi}(\mathbf{b}, q)\, \mathrm{d}\dot{a}(\mathbf{b}, q). \tag{33}$$

Here, $V_{ijk} = U_{ij,k}$, and the sensitivities of the kernels are

$$\dot{U}_{ij}(\mathbf{b}, P, Q) = U_{ij,k}(\mathbf{b}, P, Q)[\dot{x}_k(Q) - \dot{x}_k(P)], \tag{34}$$

$$\dot{W}_{ij}(\mathbf{b}, P, Q) = W_{ij,k}(\mathbf{b}, P, Q)[\dot{x}_k(Q) - \dot{x}_k(P)] \tag{35}$$

and

$$\dot{V}_{ijk}(\mathbf{b}, P, Q) = U_{ij,kn}(\mathbf{b}, P, Q)[\dot{x}_n(Q) - \dot{x}_n(P)], \tag{36}$$

where x_k are the co-ordinates of a material particle at a current configuration (at time t) and $,k = \partial/\partial x_k(Q)$. Since $\dot{x}_k(Q) - \dot{x}_k(P) \sim \mathrm{O}(r)$, $\dot{U}_{ij}$ and $\dot{W}_{ij}$ are regular and $\dot{V}_{ijk} \sim \mathrm{O}(1/r)$. Thus, differentiation with respect to b does not increase the order of the singularity.

The design derivative of the Lagrange traction rate may be expressed as

$$\dot{\tau}_i^{(L)} = n_m \dot{\sigma}_{mi} + \dot{n}_m \sigma_{mi} - \dot{n}_m g_{mi} - n_m \dot{g}_{mi} \tag{37}$$

with

$$\dot{g}_{mi} = \dot{\sigma}_{mk}\omega_{ki} + \dot{d}_{mk}\sigma_{ki} - \dot{\sigma}_{mi}\mathrm{d}_{kk} + \sigma_{mk}\dot{\omega}_{ki} + \mathrm{d}_{mk}\dot{\sigma}_{ki} - \sigma_{mi}\dot{\mathrm{d}}_{kk}. \tag{38}$$

Various quantities such as $\dot{\mathbf{x}}$, $\dot{ds}$, $\dot{da}$, $\mathbf{n}$, and $\dot{\mathbf{n}}$ must now be evaluated in order to use the above equation. These quantities can be obtained from the equations given below.

Equations for $\mathbf{F}$, $\dot{\mathbf{F}}$, $\mathrm{d}\dot{x}/\mathrm{d}x$, $\mathrm{d}\dot{s}$ *and* $\mathrm{d}\dot{a}$. Using the equations,

$$\dot{\mathbf{F}} = (\mathbf{d} + \boldsymbol{\omega}) \cdot \mathbf{F}, \quad \mathbf{F}(0) = \mathbf{I} \tag{39}$$

and

$$\dot{\mathbf{F}} = (\dot{\mathbf{d}} + \dot{\boldsymbol{\omega}}) \cdot \mathbf{F} + (\mathbf{d} + \boldsymbol{\omega}) \cdot \dot{\mathbf{F}}, \quad \dot{\mathbf{F}}(0) = \mathbf{0}, \tag{40}$$

the time histories of $\mathbf{F}$ and $\dot{\mathbf{F}}$ can be obtained by time integration of $\dot{\mathbf{F}}$ and $\ddot{\mathbf{F}}$, respectively.

Updating of the geometry of the body must be carried out, as required, during a simulation. A useful formula for determining $\mathrm{d}\dot{\mathbf{x}}/\mathrm{d}\mathbf{x}$ (i.e. $\dot{x}_{i,j}$) can be derived as follows:

$$\mathrm{d}\mathbf{x} = \mathbf{F} \cdot \mathrm{d}\mathbf{X}.$$

Therefore,

$$\mathrm{d}\dot{\mathbf{x}} = \dot{\mathbf{F}} \cdot \mathrm{d}\mathbf{X} + \mathbf{F} \cdot \mathrm{d}\dot{\mathbf{X}} \quad \text{and} \quad \frac{\mathrm{d}\dot{\mathbf{x}}}{\mathrm{d}\mathbf{x}} = \dot{\mathbf{F}} \cdot \mathbf{F}^{-1} + \mathbf{F} \cdot \frac{\mathrm{d}\dot{\mathbf{X}}}{\mathrm{d}\mathbf{X}} \cdot \mathbf{F}^{-1}$$

or, in indicial notation,

$$\dot{x}_{i,j} = \dot{F}_{iM} F^{-1}_{Mj} + F_{iM} \dot{X}_{M,K} F^{-1}_{Kj}. \tag{41}$$

Equation (41) establishes a relationship between $\dot{x}_{i,j}$ and $\dot{X}_{I,J}$. Now,

$$\mathrm{d}\dot{s} = [\dot{x}_{k,k}(Q) - n_i n_j \dot{x}_{i,j}(Q)]\,\mathrm{d}s \quad \text{and} \quad \mathrm{d}\dot{a} = \dot{x}_{k,k}(q)\,\mathrm{d}a. \tag{42, 43}$$

Design velocity $\dot{\mathbf{x}}$. There are two ways of evaluating $\dot{\mathbf{x}}$ on the boundary. The first of these is to find

$$\mathbf{v}(P) = \int_A^P \boldsymbol{\delta}\,\mathrm{d}s + \mathbf{v}(A), \qquad \dot{\mathbf{v}}(P) = \int_A^P \dot{\boldsymbol{\delta}}\,\mathrm{d}s + \int_A^P \boldsymbol{\delta}\,\mathrm{d}\dot{s} + \dot{\mathbf{v}}(A) \tag{44, 45}$$

by integration along the boundary ∂B starting at some point A on the boundary where $\mathbf{v}$ and $\dot{\mathbf{v}}$ are known. Time integration of $\mathbf{v}$ and $\dot{\mathbf{v}}$ gives $\mathbf{u}$ and $\dot{\mathbf{u}}$. Finally, at a point P on ∂B,

$$\mathbf{x} = \mathbf{X} + \mathbf{u}, \qquad \dot{\mathbf{x}} = \dot{\mathbf{X}} + \dot{\mathbf{u}}. \tag{46, 47}$$

The second approach is to find

$$\frac{\partial \dot{x}_i}{\partial s} = \dot{x}_{i,j} t_j \tag{48}$$

at a point A on ∂B. Then, one may use

$$\dot{x}_i(P) = \int_A^P \frac{\partial \dot{x}_i}{\partial s}\,\mathrm{d}s + \dot{x}_i(A). \tag{49}$$

Internal values of $\dot{\mathbf{x}}$ can be obtained by integrating $\dot{x}_{i,j}$ along lines parallel to the coordinate axes starting at boundary points with known $\dot{\mathbf{x}}$. The first approach is used in the numerical scheme presented later in this paper.

Determination of $\mathbf{n}$ *and* $\dot{\mathbf{n}}$. Using Nanson's formula,

$$\mathbf{n} \cdot \mathbf{H}\,\mathrm{d}s = \mathbf{N}\,\mathrm{d}S, \tag{50}$$

where $\mathbf{H} = \mathbf{F}/J$ and $\mathbf{N}$ is the normal in the undeformed configuration, and taking derivatives of both sides of the above equation with respect to b, one gets

$$\dot{\mathbf{n}} \cdot \mathbf{H}\,\mathrm{d}s + \mathbf{n} \cdot \dot{\mathbf{H}}\,\mathrm{d}s + \mathbf{n} \cdot \mathbf{H}\,\mathrm{d}\dot{s} = \dot{\mathbf{N}}\,\mathrm{d}S + \mathbf{N}\,\mathrm{d}\dot{S}.$$

This gives the formula

$$\dot{\mathbf{n}} = \left[-\mathbf{n} \cdot \dot{\mathbf{H}} + \dot{\mathbf{N}}\frac{\mathrm{d}S}{\mathrm{d}s}\right]\mathbf{H}^{-1} - \mathbf{n}\frac{\mathrm{d}\dot{s}}{\mathrm{d}s} + \mathbf{n}\frac{\mathrm{d}\dot{S}}{\mathrm{d}S}, \tag{51}$$

where $\mathrm{d}S/\mathrm{d}s = n_i F_{i1}/JN_1 = n_i F_{i2}/JN_2$. The values of $\mathrm{d}\dot{S}$ and $\dot{\mathbf{N}}$ in the undeformed configuration $\mathbf{X}$ can be found from formulae given by Zhang *et al.* (1992).

At the start of a time step, half of the sensitivities $\dot{\delta}_i$ and $\dot{\tau}_i^{(L)}$ are to be determined, while all the rest of the quantities in eqn (33) are known. The quantities $\tau_i^{(L)}$, δ_i, $d_{ij}^{(n)}$, and g_{mi} are known from a solution of the standard large-strain BEM problem at this time, and the sensitivity of the nonelastic deformation rates are known from differentiating a constitutive model with state variables, eqns (8) and (9), with respect to b [see Zhang (1991)].

For large-strain problems, $\tau_i^{(L)}$ and g_{mi} contain velocity gradients whose design sensitivities are not known *a priori*. Thus, like usual large-strain problems (Mukherjee and Chandra, 1987), iterations will be needed in order to solve eqn (33). The quantities $\dot{x}_{i,j}$ must be obtained from eqn (41) and used to find $\mathrm{d}\dot{s}/\mathrm{d}s$ and $\mathrm{d}\dot{a}/\mathrm{d}a$. For this, the time histories of $\mathbf{F}$ and $\dot{\mathbf{F}}$ must be tracked during the deformation process.

Stress rate and spin sensitivities on the boundary

The sensitivity equations for $\dot{\sigma}$ and $\mathbf{h}$ on ∂B are obtained by differentiating eqns (29), (30) and (7) with respect to b:

$$\mathring{\dot{\sigma}}_{ij} = A_{ijk}\dot{\tau}_k^{(C)} + B_{ijk}\dot{\delta}_k + C_{ijkl}\dot{\mathrm{d}}_{kl}^{(n)} + D_{ij}\dot{\mathrm{d}}_{kk}^{(n)} + \dot{A}_{ijk}\tau_k^{(C)} + \dot{B}_{ijk}\delta_k + \dot{C}_{ijkl}\,\mathrm{d}_{kl}^{(n)} + \dot{D}_{ij}\,\mathrm{d}_{kk}^{(n)} \tag{52}$$

$$\dot{h}_{ij} = E_{ijk}\dot{\tau}_k^{(C)} + F_{ijk}\dot{\delta}_k + G_{ijkl}\dot{d}_{kl}^{(n)} + \dot{E}_{ijk}\tau_k^{(C)} + \dot{F}_{ijk}\delta_k + \dot{G}_{ijkl}d_{kl}^{(n)} \tag{53}$$

$$\mathring{\sigma}_{ij} = \mathring{\dot{\sigma}}_{ij} - \dot{\sigma}_{ik}\omega_{kj} - \sigma_{ik}\dot{\omega}_{kj} + \dot{\omega}_{ik}\sigma_{kj} + \omega_{ik}\dot{\sigma}_{kj}. \tag{54}$$

Sensitivity equations at an internal point

This equation is obtained by differentiating eqn (31) with respect to b and may be written as

$$\begin{aligned}
\dot{h}_{jf}(\mathbf{b},p) = &\int_{\partial B} [V_{ijf}(\mathbf{b},p,Q)\dot{\tau}_i^{(L)}(\mathbf{b},Q) - Y_{ijf}(\mathbf{b},p,Q)\dot{\delta}_i(\mathbf{b},Q)]\,\mathrm{d}s(\mathbf{b},Q)\\
&+\int_{\partial B} [\dot{V}_{ijf}(\mathbf{b},p,Q)\tau_i^{(L)}(\mathbf{b},Q) - \dot{Y}_{ijf}(\mathbf{b},p,Q)\delta_i(\mathbf{b},Q)]\,\mathrm{d}s(\mathbf{b},Q)\\
&+\int_{\partial B} [V_{ijf}(\mathbf{b},p,Q)\tau_i^{(L)}(\mathbf{b},Q) - Y_{ijf}(\mathbf{b},p,Q)\delta_i(\mathbf{b},Q)]\,\dot{\mathrm{d}}s(\mathbf{b},Q)\\
&-2G\dot{d}_{ik}^{(n)}(\mathbf{b},p)\int_{\partial B} V_{ijk}(\mathbf{b},p,Q)n_l(\mathbf{b},Q)\,\mathrm{d}s(\mathbf{b},Q)\\
&-2Gd_{ik}^{(n)}(\mathbf{b},p)\int_{\partial B} \dot{V}_{ijk}(\mathbf{b},p,Q)n_l(\mathbf{b},Q)\,\mathrm{d}s(\mathbf{b},Q)\\
&-2Gd_{ik}^{(n)}(\mathbf{b},p)\int_{\partial B} V_{ijk}(\mathbf{b},p,Q)\dot{n}_l(\mathbf{b},Q)\,\mathrm{d}s(\mathbf{b},Q)\\
&-2Gd_{ik}^{(n)}(\mathbf{b},p)\int_{\partial B} V_{ijk}(\mathbf{b},p,Q)n_l(\mathbf{b},Q)\,\dot{\mathrm{d}}s(\mathbf{b},Q)\\
&-\dot{g}_{mi}(\mathbf{b},p)\int_{\partial B} V_{ijm}(\mathbf{b},p,Q)n_l(\mathbf{b},Q)\,\mathrm{d}s(\mathbf{b},Q)\\
&-g_{mi}(\mathbf{b},p)\int_{\partial B} \dot{V}_{ijm}(\mathbf{b},p,Q)n_l(\mathbf{b},Q)\,\mathrm{d}s(\mathbf{b},Q)\\
&-g_{mi}(\mathbf{b},p)\int_{\partial B} V_{ijm}(\mathbf{b},p,Q)\dot{n}_l(\mathbf{b},Q)\,\mathrm{d}s(\mathbf{b},Q)\\
&-g_{mi}(\mathbf{b},p)\int_{\partial B} V_{ijm}(\mathbf{b},p,Q)n_l(\mathbf{b},Q)\,\dot{\mathrm{d}}s(\mathbf{b},Q)
\end{aligned}$$

$$
\begin{aligned}
&- \int_B 2G\dot{P}_{ijkl}(\mathbf{b},p,q)[d_{ik}^{(n)}(\mathbf{b},q) - d_{ik}^{(n)}(\mathbf{b},p)]\,da(\mathbf{b},q) \\
&+ \int_B 2GP_{ijkl}(\mathbf{b},p,q)[\dot{d}_{ik}^{(n)}(\mathbf{b},q) - \dot{d}_{ik}^{(n)}(\mathbf{b},p)]\,da(\mathbf{b},q) \\
&+ \int_B 2GP_{ijkl}(\mathbf{b},p,q)[d_{ik}^{(n)}(\mathbf{b},q) - d_{ik}^{(n)}(\mathbf{b},p)]\,d\dot{a}(\mathbf{b},q) \\
&+ \int_B \dot{P}_{ijml}(\mathbf{b},p,q)[g_{mi}(\mathbf{b},q) - g_{mi}(\mathbf{b},p)]\,da(\mathbf{b},q) \\
&+ \int_B P_{ijml}(\mathbf{b},p,q)[\dot{g}_{mi}(\mathbf{b},q) - \dot{g}_{mi}(\mathbf{b},p)]\,da(\mathbf{b},q) \\
&+ \int_B P_{ijml}(\mathbf{b},p,q)[g_{mi}(\mathbf{b},q) - g_{mi}(\mathbf{b},p)]\,d\dot{a}(\mathbf{b},q), \qquad (55)
\end{aligned}
$$

where $Y_{ijl} = W_{ij,l}$ and $P_{ijkl} = U_{ij,kl}$.

Although eqn (55) is long, it may be easily evaluated. The boundary kernels are regular and the domain integrands are $1/r$ singular. These domain integrals can be accurately evaluated by standard means [e.g. Mukherjee (1982)]. The entire right-hand side of eqn (55) is known at this stage except for the integrals involving $\dot{g}_{mi}$, which depend on $\dot{h}_{ij}$. Accordingly, iterations are needed over eqns (33) and (55). These iterations are similar to those needed over velocity gradients for BEM analyses of large-strain problems.

Stress rate sensitivities at an internal point

Finally, the sensitivities $\dot{\sigma}$ at an internal point are evaluated from a differentiated form of the hypoelastic law [eqn (6)] with respect to b,

$$
\dot{\sigma}_{ij}^{\cdot} = \lambda \dot{h}_{kk}\delta_{ij} + G(\dot{h}_{ij} + \dot{h}_{ji}) - 2G\dot{d}_{ij}^{(n)} \qquad (56)
$$

together with eqn (54) for $\dot{\delta}_{ij}$.

It should be noted here that the sensitivity equations from this formulation are nonlinear, as are the equations governing the standard problem. The stiffness matrices of the discretized forms of the sensitivity and standard equations, however, turn out to be identical. This aspect is discussed further in the section entitled "Numerical Implementation".

MODELING OF SHARP CORNERS ON ∂B

The modeling of sharp corners has been discussed in detail by Zhang and Mukherjee (1991a) for the elastic case and by Zhang *et al.* (1992) for elasto–plastic problems. Two kinds of situations can arise: (a) special corners across which the Cauchy stress tensor σ remains continuous throughout a deformation process and (b) general corners across which σ can suffer a jump discontinuity. It is also possible for σ to become unbounded at a corner, but such situations are not considered in this work. The plane strain problem is considered below.

In certain special situations, the Cauchy stress tensor (and therefore its material rate) remains continuous at a corner throughout the deformation history. An example is a right-angled corner in which the corner angle remains a right angle throughout a deformation process. Another example is a corner that arises from using symmetry in a problem where the point was originally regular. In such cases, one can write corner equations in a manner analogous to the cases that have been considered before by Zhang and Mukherjee (1991a) and Zhang *et al.* (1992):

$$\dot{\sigma}_{ij}^{-} = \dot{\sigma}_{ij}^{+}, \tag{57}$$

where $\dot{\sigma}_{ij}$, on either side of the corner, is obtained from eqns (7), (29) and (30) [together with (4)], as functions of components of $\boldsymbol{\tau}^{(c)}$, $\boldsymbol{\delta}$, $\mathbf{d}^{(n)}$ and $\boldsymbol{\sigma}$, as well as v, G, $\mathbf{n}$ and $\mathbf{t}$. In this case, the corner sensitivity equation is of the form

$$\dot{\sigma}_{ij}^{-} = \dot{\sigma}_{ij}^{+}. \tag{58}$$

A possible option for the general case is to invoke continuity of the velocity $\mathbf{v}$ at a corner. This leads to integral constraints as shown below. Suppose that AC and CB are two smooth segments that meet at corner C. Then, continuity of $\mathbf{v}$ at C demands that

$$v_i(P) + \int_P^C \delta_i^{-}\, \mathrm{d}s = v_i(Q) - \int_C^Q \delta_i^{+}\, \mathrm{d}s, \tag{59}$$

where P within AC and Q within CB are points at which the velocities are known. Of course, if velocities are not known at any point within smooth segments contiguous to a corner, then velocity information from points farther away must be used and eqn (59) must be suitably modified. Knowledge of $\mathbf{v}$ at any one point on ∂B is sufficient for this idea to work.

Equation (59) gives two equations at each corner, and this extra information is sufficient to solve the problem. The sensitivity equation corresponding to (59) has the form

$$\dot{v}_i(P) + \int_P^C \dot{\delta}_i^{-}\, \mathrm{d}s + \int_P^C \delta_i^{-}\, \mathrm{d}\dot{s} = \dot{v}_i(Q) - \int_C^Q \dot{\delta}_i^{+}\, \mathrm{d}s - \int_C^Q \delta_i^{+}\, \mathrm{d}\dot{s}. \tag{60}$$

A word of caution here. Sometimes, as discussed in detail by Zhang and Mukherjee (1991a), Δ_n and associated rotations can become singular at a corner. In such cases, care must be exercised in using eqns (59) and (60) in the general case. Suitable shape functions for Δ_n must be employed to reflect this singular behavior.

NUMERICAL IMPLEMENTATION

Discretization of equations

The discretization procedure is quite standard and is similar to that used for small-strain elasto–viscoplastic problems (Zhang *et al.*, 1992). For plane strain problems, the DBEM equations (27) and (31) and the sensitivity equations (33) and (55) must be discretized. Of course, the corresponding equations from Zhang (1991) must be used for plane stress problems.

The boundary of the body ∂B is subdivided into piecewise quadratic, conforming boundary elements. The variables $\boldsymbol{\tau}^{(L)}$ and $\boldsymbol{\delta}$, their sensitivities $\dot{\boldsymbol{\tau}}^{(L)}$ and $\dot{\boldsymbol{\delta}}$, and the scalar $\mathrm{d}\dot{s}/\mathrm{d}s$ are assumed to be piecewise quadratic on the boundary elements. The domain of the body is divided into Q4 internal cells. The tensors $\mathbf{d}^{(n)}$ and $\mathbf{g}$, their sensitivities, and the scalar $\mathrm{d}\dot{a}/\mathrm{d}a$ are interpolated on these internal cells.

As has been mentioned before, singular integrals must be evaluated with great care for these problems. Logarithmically singular integrands are integrated with log-weighted Gaussian integration formulae on the boundary elements. The $1/r$ singular domain integrals are first transformed into regular ones by mapping (Mukherjee, 1982, pp. 91–92) and then evaluated by regular Gaussian quadrature on a square. The number of Gauss points used for regular and log-singular boundary integrals are 20 and 16, respectively. For regular domain integrals, as well as $1/r$ singular domain integrals which are transformed to regular form, the number of Gauss points used is 3×3.

When corners exist on $\hat{c}B$, the corner equations are added to the usual DBEM equations (22) and (33) and all the equations are assembled together. The resulting systems of boundary equations are of the form

$$[A]\{\delta\}+[B]\{\tau^{(L)}\} = \{C_1\} \tag{61}$$

and

$$[A]\{\dot{\delta}\}+[B]\{\dot{\tau}^{(L)}\} = \{C_2\}, \tag{62}$$

where the right-hand sides of the equations contain contributions from the last two integrals of eqn (27) and the last eight integrals of eqn (33). It is important to note that $\{\tau^{(L)}\}$ and $\{C_1\}$ contain the unknown velocity gradients **h** through the tensor **g** [and similarly for the discretized sensitivity equation (62)], so that iterations, within each time step, now become necessary. Details of this procedure are given in the next section. Another important fact is that the coefficient matrices $[A]$ and $[B]$ are identical in eqns (61) and (62). Internal point equations (31) and (55) are discretized in a similar fashion.

Solution strategy

The solution algorithm for large-strain elasto–viscoplastic problems, which involves solutions of appropriate equations at the beginning of each time step and then marching forward in time, is discussed in detail in several papers (Chandra and Mukherjee, 1983; Mukherjee and Chandra, 1987). Iterations are needed, since the velocity gradients appearing in eqn (27) (in a domain integral and in the boundary integral through $\tau_i^{(L)}$) are not known *a priori*. One important advantage of this DBEM formulation over the usual BEM formulation (Mukherjee and Chandra, 1987) is that velocity components do not appear, by themselves, in these equations and that the boundary velocity gradients can be directly evaluated from eqn (30).

Sensitivity calculations must also be carried out using a procedure analogous to that of the usual large-strain problem. Also, this must be done in parallel with the usual problem. Iterations over sensitivities of velocity gradients are now needed.

Another important difference between the usual large deformation simulation and the sensitivity analysis of large deformation problems is that not only the body geometry but also the design quantities, such as $\dot{x}_i$, $\mathrm{d}\dot{s}/\mathrm{d}s$ and $\mathrm{d}\dot{a}/\mathrm{d}a$, need to be updated during the simulation.

The algorithm (for the sensitivity problem) for going from time t to $t+\Delta t$ is illustrated in Fig. 2. The complete solution strategy is as follows:

(1) Solve the elasticity problem to obtain the initial (time zero) solutions for Δ_i, τ_i, σ_{ij}, $u_{i,j}$, u_i and $\dot{\Delta}_i$, $\dot{\tau}_i$, $\dot{\sigma}_{ij}$, $\dot{u}_{i,j}$, $\dot{u}_i$. Usually, one starts from a zero elastic solution.
(2) Obtain the tensors $d_{ik}^{(n)}$ and $\dot{d}_{ik}^{(n)}$ from the constitutive equations and the derivatives of the constitutive equations.
(3) Solve the DBEM equations for the standard problem.
  (3.1) If $t = 0$, assume $h_{ij} = 0$. Otherwise use value from previous time.
  (3.2) Solve eqn (27) with estimated values of $\tau_i^{(L)}$ and prescribed values of δ_i on the boundary.
  (3.3) Use the boundary algebraic equation (30) to determine h_{ij} on the boundary.
  (3.4) Solve eqn (31) for h_{ij} at selected internal points.
  (3.5) Check convergence of h_{ij}. If it is not satisfied, use the calculated value of h_{ij} as the new estimated value and go to step (3.2).
(4) Solve the DBEM equations for the sensitivity problem.
  (4.1) If $t = 0$, assume $\dot{h}_{ij} = 0$. Otherwise use value from previous time.
  (4.2) Solve eqn (33) with estimated values of $\dot{\tau}_i^{(L)}$ and prescribed values of $\dot{\delta}_i$ on the boundary.

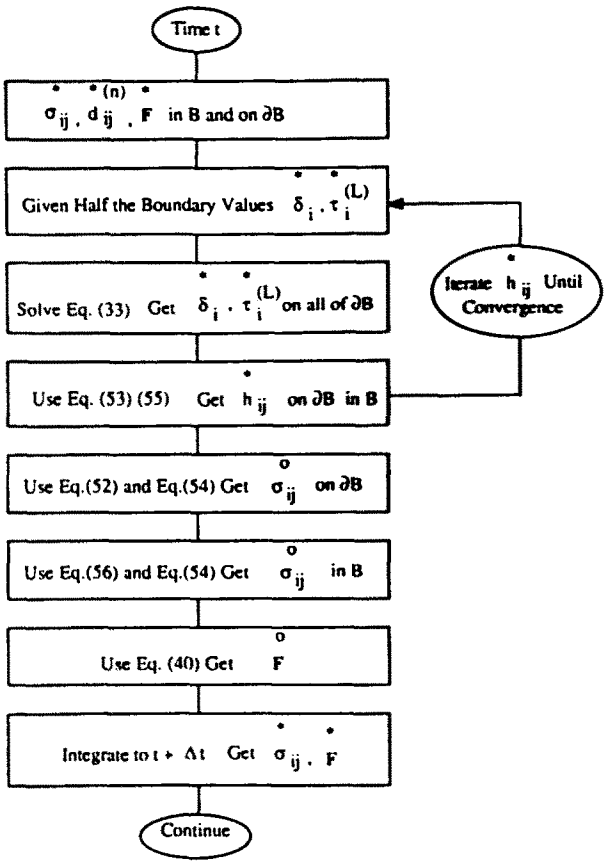

Fig. 2. Solution strategy for large deformation problems.

(4.3) Use the boundary algebraic equation (53) to determine $\dot{h}_{ij}$ on the boundary.
(4.4) Solve eqn (55) for $\dot{h}_{ij}$ at selected internal points.
(4.5) Check convergence of $\dot{h}_{ij}$. If it is not satisfied, use the calculated value of $\dot{h}_{ij}$ as the new estimated value and go to step (4.2).

(5) Calculate boundary values of $\dot{\sigma}_{ij}$ and $\dot{\sigma}_{ij,j}$, as well as $\overset{\circ}{\dot{\sigma}}_{ij}$ and $\dot{\sigma}_{ij,j}$, from eqns (29), (7), (52) and (54), respectively.

(6) Calculate internal values of $\dot{\sigma}_{ij}$ and $\dot{\sigma}_{ij,j}$, as well as $\overset{\circ}{\dot{\sigma}}_{ij}$ and $\dot{\sigma}_{ij,j}$, from eqns (32), (7), (56) and (53), respectively.

(7) Obtain v_i and $\dot{v}_i$ on the boundary ∂B by integrating δ_i and $\dot{\delta}_i$ along the boundary using eqns (44)–(45) (at time zero, $\mathrm{d}\dot{s}/\mathrm{d}s = \mathrm{d}\dot{S}/\mathrm{d}S$). The internal values of v_i can be obtained by integrating h_{ij} along lines parallel to the x_1 and x_2 axes starting at boundary points where v_i are known.

(8) Use eqns (39) and (40) to calculate $\dot{\mathbf{F}}$ and $\overset{\circ}{\dot{\mathbf{F}}}$.

(9) Integrate the rate quantities $\dot{\sigma}_{ij}$, $\overset{\circ}{\dot{\sigma}}_{ij}$, v_i, $\dot{v}_i$, $\dot{\mathbf{F}}$ and $\overset{\circ}{\dot{\mathbf{F}}}$ in time to obtain σ_{ij}, $\overset{\circ}{\dot{\sigma}}_{ij}$, u_i, $\dot{u}_i$, $\mathbf{F}$ and $\dot{\mathbf{F}}$ at $t+\Delta t$. The displacement sensitivity components $\dot{u}_i$ are available only on the boundary. The other quantities are available both on the boundary and in the domain.

(10) Determine if the geometry of the body needs to be updated. If the answer is yes, go to the next step; otherwise, go to step (2) until the simulation ends.

(11) Update the geometry of the body.
(11.1) Use eqn (41) to obtain $\dot{x}_{i,j}$ first.
(11.2) Determine $\mathrm{d}\dot{s}$ and $\mathrm{d}\dot{a}$ on the new geometry from eqns (42) and (43).
(11.3) Calculate x_i (both on ∂B and in B) and $\dot{x}_i$ (only on ∂B) from eqns (46) and (47).

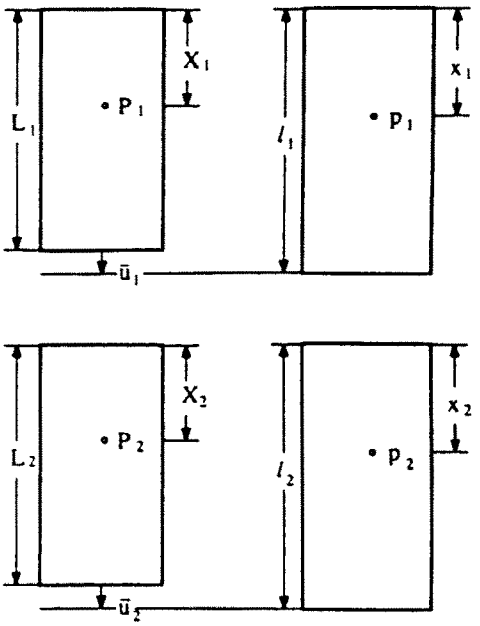

Fig. 3. Illustrative one-dimensional problem.

(11.4) The internal values of $\dot{x}_i$ can be calculated by integrating $\dot{x}_{i,j}$ along lines parallel to the x_1 and x_2 axes starting at boundary points where $\dot{x}_i$ are known.

(11.5) Update all the kernels and derivatives of the kernels that appear in eqns (27), (31), (33) and (55) and go to step (2).

For classical elastic–plastic material models, $\dot{d}_{ij}^{(n)}$ depends on $\dot{\bar{\sigma}}_{ij}$, as well as on the stress components and their sensitivities. This requires iterations over $\dot{d}_{ij}^{(n)}$ within each time step. The sensitivity problem, however, still has approximately the same level of complexity as the original elastic–plastic problem. For large-strain problems, iterations over $\dot{d}_{ij}^{(n)}$ may be carried out within the iteration scheme for $\dot{h}_{ij}$.

Thus, large-strain sensitivity problems of elasto–plasticity and elasto–viscoplasticity are expected to require less than twice the computational effort needed for the regular BEM analysis including both geometric and material nonlinearities when sensitivity with respect to one design variable is needed. In a typical design environment, however, sensitivities with respect to a large number of design variables are desired. It is interesting to note here that the determination of sensitivities with respect to additional design variables does not require solutions of new matrix systems. The coefficient matrices remain the same for all cases, only the right-hand sides change. Hence, for the slight increase in additional costs due to additional evaluations of the right-hand side, it is possible to simultaneously track the sensitivities with respect to several design variables.

ILLUSTRATIVE ONE-DIMENSIONAL PROBLEMS

The problem

The example considered here is a rectangular plate of initial length L, of unit width. The problem can be plane strain or plane stress. The plate is deformed to a current length l by a prescribed displacement history $\bar{u}$.

Figure 3 shows two such plates of initial lengths L_1 and L_2. A generic material point X_1, in this simple one-dimensional situation, moves to x_1 and X_2 moves to x_2, where

$$x_1 = \frac{l_1}{L_1} X_1 \quad \text{and} \quad x_2 = \frac{l_2}{L_2} X_2. \tag{63, 64}$$

The *design deformation* $X_1 \to X_2$ is assumed to be of the form

$$X_2 = X_1 \frac{L_2}{L_1}. \tag{65}$$

As discussed by Zhang *et al.* (1992), the above expression for the design deformation at an internal point is not unique. However, such an assumption only affects sensitivities inside a body, not on its boundary.

As a consistency check, one can write

$$\dot{x} = \frac{\mathrm{d}x}{\mathrm{d}X_\mathrm{D}} \cdot \frac{\mathrm{d}X_\mathrm{D}}{\mathrm{d}L}, \tag{66}$$

where L is the design variable. It is easy to show that

$$\frac{\mathrm{d}x}{\mathrm{d}X_\mathrm{D}} = \lim_{\Delta X \to 0} \frac{x_2 - x_1}{X_2 - X_1} = 1 + \dot{\tilde{u}}, \qquad \frac{\mathrm{d}X_\mathrm{D}}{\mathrm{d}L} = \lim_{\Delta L \to 0} \frac{X_2 - X_1}{L_2 - L_1} = \frac{X}{L}, \tag{67, 68}$$

so that, from eqn (66),

$$\dot{x} = \frac{X}{L}(1 + \dot{\tilde{u}}). \tag{69}$$

Now,

$$\dot{u} = \lim_{\Delta L \to 0} \frac{u_2 - u_1}{L_2 - L_1} = \frac{X}{L}\dot{\tilde{u}}, \quad \text{so that} \quad \dot{x} = \dot{X} + \dot{u}$$

as expected. Also,

$$\dot{l} = 1 + \dot{\tilde{u}}.$$

Consistency check of formulae for $\dot{\mathbf{F}}$, $\mathring{\mathbf{F}}$, $\mathrm{d}\dot{x}/\mathrm{d}x$, $\mathrm{d}\mathring{s}$ *and* $\mathrm{d}\mathring{a}$ *for one-dimensional strain*

A one-dimensional strain problem is a plane strain problem with only a single component of the displacements at every point in the body. Let this component be the displacement in the x_1 direction. The only nonzero components of $\mathbf{F}$ and $\mathbf{d}$, therefore, are

$$F_{11} = \frac{l}{L} \quad \text{and} \quad d_{11} = \frac{v}{l}. \tag{70, 71}$$

Now,

$$\dot{F}_{11} = \frac{v}{L}, \qquad \mathring{F}_{11} = \frac{\dot{l}}{L} - \frac{l}{L^2} \quad \text{and} \quad \mathring{d}_{11} = \frac{\dot{v}}{l} - \frac{v}{l^2}\dot{l}. \tag{72, 73 and 74}$$

In the above, v is the velocity component in the 1-direction. Also, $\omega = 0$. From eqns (63) and (69),

$$\dot{x}_1 = \dot{x} = \frac{x}{l}(1 + \dot{\tilde{u}}). \tag{75}$$

Various formulae presented before can now be easily checked for this simple one-dimensional case. Equation (39) for $\dot{\mathbf{F}}$ is obviously valid. The right- and left-hand sides of eqn (40) become $\dot{v}/L - v/L^2$.

The formula (41) for $\dot{x}_{i,j}$ with $\mathrm{d}\dot{X}/\mathrm{d}X = 1/L$, gives

$$\frac{\mathrm{d}\overset{*}{x}}{\mathrm{d}x} = \overset{*}{x}_{1,1} = \frac{1+\overset{*}{u}}{l}$$

which is consistent with eqn (75).

From eqns (42) and (43) ($\mathrm{d}\overset{*}{s}/\mathrm{d}s$ is evaluated on edges parallel to the x_1 axis),

$$\frac{\mathrm{d}\overset{*}{s}}{\mathrm{d}s} = \frac{1+\overset{*}{u}}{l}, \quad \frac{\mathrm{d}\overset{*}{a}}{\mathrm{d}a} = \frac{1+\overset{*}{u}}{l}$$

which are correct since, in this case, s can be identified with x, i.e. [see eqn (75)]

$$\overset{*}{s} = \frac{s}{l}(1+\overset{*}{u}).$$

Illustrative constitutive model

The DBEM formulation presented in this paper is quite general, and any of a large number of elasto–viscoplastic constitutive models can be used here to describe material behavior. The reader is referred to Mukherjee (1982) for a discussion of such models.

The particular model chosen for the numerical results discussed in this paper is due to Anand (1982). This is a unified elasto–viscoplastic model with a single scalar internal variable s. The model, adapted to the present multi-axial situation, is described by the equation

$$d^{(n)}_{ij} = \frac{3d^{(n)}}{2\sigma}\sigma'_{ij}, \tag{76}$$

where σ'_{ij} are the components of the deviatoric part of the Cauchy stress and σ is the stress invariant defined as

$$\sigma = \sqrt{\tfrac{3}{2}\sigma'_{ij}\sigma'_{ij}}.$$

The invariant $d^{(n)}$ is given by the equation

$$d^{(n)} = A\,\mathrm{e}^{-Q/KT}\left(\frac{\sigma}{s}\right)^{1/m} \tag{77}$$

together with the evolution equation

$$\dot{s} = h_0\left(1-\frac{s}{s_c}\right)d^{(n)}, \tag{78}$$

where

$$s_c = s_a\left[\frac{d^{(n)}}{A}\,\mathrm{e}^{Q/KT}\right]^n.$$

Here, T is the temperature in degrees Kelvin, Q is the activation energy and K is the Boltzmann constant. Also, A, h_0, s_a, m and n are material constants of which m and n are, in general, temperature dependent. The particular parameters used here are representative of F_e–0.05 carbon steel in a temperature range of 1173–1573 K and strain rate range of $1.4\times10^{-4}\ \mathrm{s}^{-1}$ to $2.3\times10^{-2}\ \mathrm{s}^{-1}$. These parameters have been used for all the isothermal simulations (at $T = 1173$ K) reported here. They are

$$A = 10^{11}\ \mathrm{s}^{-1}, \quad h_0 = 1329.22\ \mathrm{MPa},$$
$$s_a = 147.6\ \mathrm{MPa}, \quad m = 0.147,$$
$$n = 0.03, \quad Q/K = 3.28 \times 10^4\ \mathrm{K},$$

together with elastic constants (at 1173 K)

$$G = 2.2615 \times 10^3\ \mathrm{MPa}, \quad \nu = 0.3.$$

Also, the initial value of the state variable s is 47.11 MPa and the initial value of the sensitivity $\overset{*}{s}$ is zero.

Numerical examples

A computer program for numerically calculating sensitivities for general two-dimensional (plane strain or plane stress) problems has been developed. It is crucial that results from such a computer program be carefully checked against analytical (or direct) solutions for simple geometrical situations. The problems described here are a one-dimensional strain problem in which the only nonzero displacement is u_1 and a one-dimensional stress problem with the only nonzero stress σ_{11}. The plane strain version of the *two-dimensional* DBEM computer program is employed to solve the one-dimensional strain problem, while the plane stress version is used to solve the one-dimensional stress problem. In both cases, a constant velocity $v_0 = 2 \times 10^{-3}\ \mathrm{m\ s}^{-1}$ is applied in the x_1 direction with a very small value of initial strain in this direction. The design variable is the initial length L in the x_1 direction. The initial dimensions of the plate are 2 m × 2 m. The constant time step Δt for explicit time integration is 0.01 s. These tests serve to verify the methodology and the algorithm of the DBEM approach, especially the updating of the geometry as well as quantities such as $\dot{x}$, $\mathrm{d}\overset{*}{s}/\mathrm{d}s$, and $\mathrm{d}\overset{*}{a}/\mathrm{d}a$ during a simulation. These quantities are updated every second in these simulations.

Direct solution for the one-dimensional strain problem. A direct solution is obtained by time integration of the one-dimensional equations. For the one-dimensional strain problem being considered here,

$$v_{1,1} = d_{11} = v_0/l, \quad \text{rest of } v_{i,j} = 0, \quad \omega_{ij} = 0.$$

From the hypoelastic law (6) [and eqn (7)],

$$\dot{\sigma}_{11} = \hat{\sigma}_{11} = \frac{2(1-\nu)}{1-2\nu} G \frac{v_0}{l} - 2G d_{11}^{(n)}, \tag{79}$$

$$\dot{\sigma}_{22} = \hat{\sigma}_{22} = \frac{2\nu}{1-2\nu} G \frac{v_0}{l} - 2G d_{22}^{(n)}, \qquad \dot{\sigma}_{33} = \dot{\sigma}_{22}. \tag{80, 81}$$

The rest of the stress rates vanish.

For the corresponding sensitivity equations,

$$\overset{*}{\dot{u}} = 0, \quad \overset{*}{l} = 1, \quad \mathrm{d}\overset{*}{s}/\mathrm{d}s = 1/l, \quad \mathrm{d}\overset{*}{a}/\mathrm{d}a = 1/l$$

and

$$\overset{*}{\dot{\sigma}}_{11} = -\frac{2(1-\nu)}{1-2\nu} G \frac{v_0}{l^2} - 2G \overset{*}{d}_{11}^{(n)}, \qquad \overset{*}{\dot{\sigma}}_{22} = -\frac{2\nu}{1-2\nu} G \frac{v_0}{l^2} - 2G \overset{*}{d}_{22}^{(n)}, \qquad \overset{*}{\dot{\sigma}}_{33} = \overset{*}{\dot{\sigma}}_{22}. \tag{82–84}$$

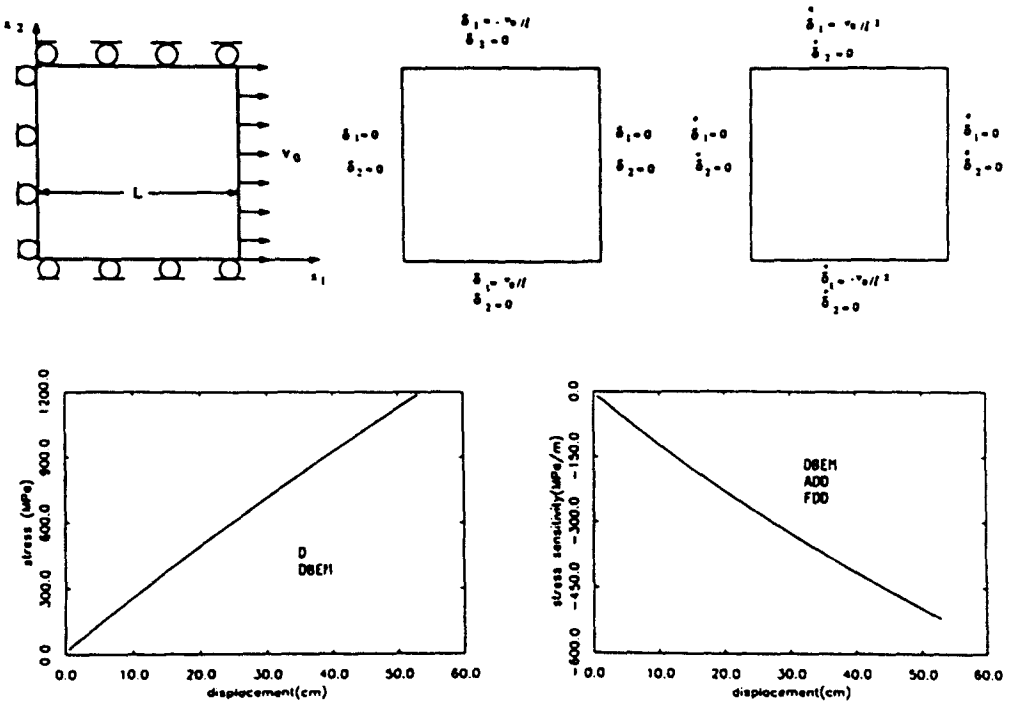

Fig. 4. Results for 1-D strain. $v_0 = 2 \times 10$ (m s^{-1}). FDD: Finite difference of direct solutions; D: Direct; DBEM: Derivative BEM; ADD: Analytical differentiation of direct solutions.

The quantities $\mathbf{d}^{(n)}$ and $\dot{\mathbf{d}}^{(n)}$ are obtained from the constitutive equations (76)–(78) together with the derivatives of these equations with respect to the design variable L. These sensitivity equations, derived from the above constitutive model, are given in Zhang (1991). Similar equations can be easily derived for the one-dimensional stress problem.

Numerical results. The physical situation, as well as the results, are shown in Figs 4 and 5. The boundary conditions, in terms of the rate quantities and their sensitivities, also appear in Figs 4 and 5. The DBEM model has nonstandard boundary variables, and these must be prescribed such that a unique solution is obtained (Zhang *et al.*, 1992).

Figure 4 shows the stress-dependent plot in the x_1 direction (σ_{11} as a function of u_1) and the corresponding sensitivity plot ($\dot{\sigma}_{11}$ versus u_1) for the one-dimensional strain problem. The displacement is the abscissa since, in these examples, the velocity, rather than the strain rate, is kept constant and insensitive to the design variable L. Also, "D" refers to the direct solution, "FDD" to the finite difference of direct solutions, and "ADD" to the analytical differentiation of a direct solution. The direct solution is a time-marching solution obtained by integrating the one-dimensional equations given in the previous section. The FDD solution is obtained with $\Delta L = 0.001$. The DBEM numerical results are obtained employing four quadratic boundary elements (one for each edge) and four internal Q4 elements with one internal point at the center of the plate.

The corresponding situation for one-dimensional stress problems is depicted in Fig. 5. The DBEM numerical solutions on the four plots are seen to agree almost perfectly with the direct solutions, which can be regarded as semi-analytical solutions of the problems. From a practical point of view, the one-dimensional strain problem is somewhat unrealistic in that it is over-constrained and requires very large stresses for the deformation shown in Fig. 4. However, this example serves as a good check for the computer program.

It is interesting to note that the sensitivity plot for the one-dimensional stress problem is considerably more complicated than the corresponding plot for the one-dimensional strain problem. The first oscillation (at low strain) in the sensitivity plot in Fig. 5 is due to

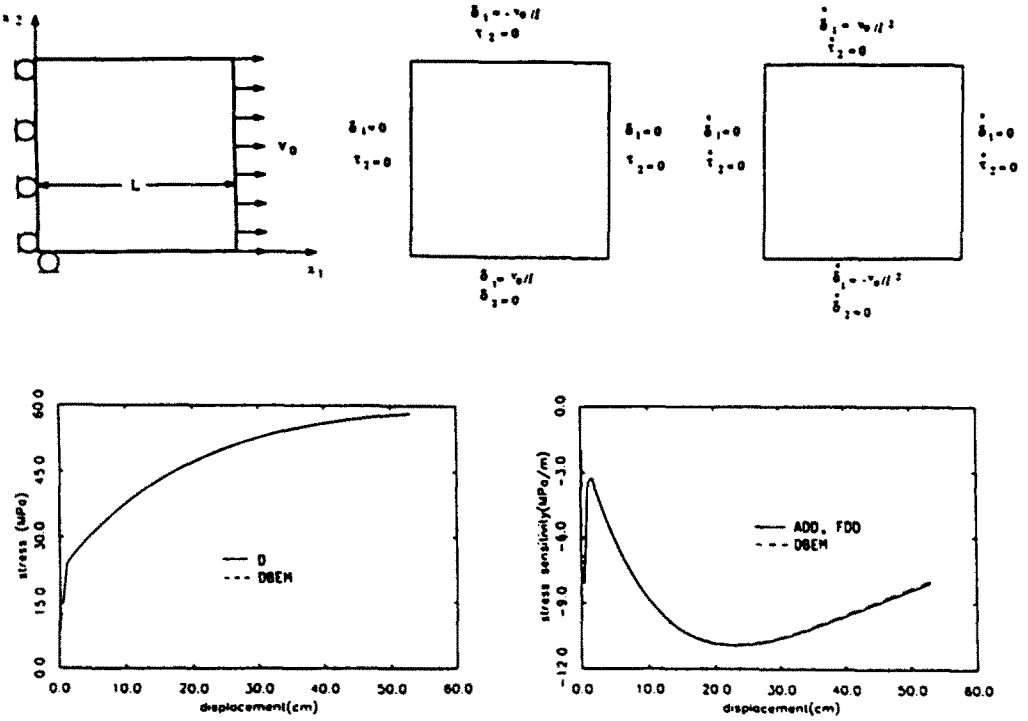

Fig. 5. Results for 1-D stress. $v_0 = 2 \times 10$ (m s^{-1}). FDD: Finite difference of direct solutions; D: Direct; DBEM: Derivative BEM; ADD: Analytical differentiation of direct solutions.

the elastic–plastic transition. The reasons for this are discussed in detail in the paper on sensitivities in small-strain elasto–plastic problems (Zhang *et al.*, 1992).

CONCLUSIONS

The first results for DSCs for solid continua undergoing large deformation, obtained by direct analytical differentiation of the relevant boundary integral equations, are presented in this paper. The elastic strains in these deforming solids are assumed to be small, but the nonelastic strains and rotations can be arbitrarily large.

The DSCs, for this class of strongly nonlinear problems, are history dependent. Also, the demands on the accuracy of solutions for these problems are very high. Thus, although these first numerical examples have simple geometry, it is very encouraging to see that the DSCs are obtained accurately over the entire history of the deformation process.

DSCs are useful in diverse applications. The primary goal of this ongoing research program is the optimal design of nonlinear processes—primarily manufacturing processes—in solid mechanics. Thus, it is expected that the approach for sensitivity calculations presented here will prove to be very useful for problems such as the design of optimal die shapes for extrusion or optimal pre-form shapes for forging. Such problems are extremely challenging, but potential rewards from solving these problems are expected to be very substantial.

Acknowledgements—This research has been supported by NSF grant number MSS-8922185 to Cornell University and The University of Arizona. All computing for this research has been performed at the Cornell National Supercomputer Facility.

REFERENCES

Aithal, R., Saigal, S. and Mukherjee, S. (1991). Three-dimensional boundary element implicit differentiation formulation for design sensitivity analysis. *Math. Comput. Model.* **15**, 1–10.

Anand, L. (1982). Constitutive equations for the rate-dependent deformation of metals at elevated temperatures. *ASME J. Engng Mater. Tech.* **104**, 12–17.

Ang, A. H.-S. and Tang, W. H. (1975). *Probability Concepts in Engineering Planning and Design*. Wiley, New York.

Barone, M. R. and Yang, R.-J. (1988). Boundary integral equations for recovery of design sensitivities in shape optimization. *AIAA Jl* **26**, 589–594.

Barone, M. R. and Yang, R.-J. (1989). A boundary element approach for recovery of shape sensitivities in three-dimensional elastic solids. *Comput. Meth. Appl. Mech. Engng* **74**, 69–82.

Cardoso, J. B. and Arora, J. S. (1988). Variational methods for design sensitivity analysis in nonlinear structural mechanics. *AIAA Jl* **26**, 595–602.

Chandra, A. and Mukherjee, S. (1983). Applications of the boundary element method to large strain-large deformation problems of viscoplasticity. *J. Strain Anal.* **8**, 261–270.

Chandra, A. and Mukherjee, S. (1986). An analysis of large strain viscoplasticity problems including the effects of induced material anisotropy. *ASME J. Appl. Mech.* **53**, 77–82.

Choi, J. H. and Choi, K. K. (1990). Direct differentiation method for shape design sensitivity analysis using boundary integral formulation. *Comput. Struct.* **34**, 499–508.

Choi, K. K. and Santos, J. L. T. (1987). Design sensitivity analysis of nonlinear structural systems; part I: theory. *Int. J. Num. Meth. Engng* **24**, 2039–2055.

Cruse, T. A. and Vanburen, W. (1971). Three-dimensional elastic stress analysis of a fracture specimen with an edge crack. *Int. J. Fract. Mech.* **7**, 1–15.

Fung, Y. C. (1965). *Foundations of Solid Mechanics*. Prentice-Hall, Englewood Cliffs, NJ.

Ghosh, N. and Mukherjee, S. (1987). A new boundary element method formulation for three-dimensional problems in linear elasticity. *Acta Mech.* **67**, 107–199.

Ghosh, N., Rajiyah, H., Ghosh, S. and Mukherjee, S. (1986). A new boundary element method formulation for linear elasticity. *ASME J. Appl. Mech.* **53**, 69–76.

Haug, E. J., Choi, K. K. and Komkov, V. (1986). *Design Sensitivity Analysis of Structural Systems*. Academic Press, New York.

Huang, Q. and Du, Q. (1988). An improved formulation for domain stress evaluation by boundary element methods in elastoplastic problems. *Proceedings, China U.S. Seminar on Boundary Integral Equations and Boundary Finite Element Methods in Physics and Engineering*, Xian, China.

Kane, J. H. and Saigal, S. (1988). Design sensitivity analysis of solids using BEM. *ASCE J. Engng Mech.* **114**, 1703–1722.

Mukherjee, S. (1982). *Boundary Element Methods in Creep and Fracture*. Elsevier, London.

Mukherjee, S. and Chandra, A. (1987). Nonlinear solid mechanics. In *Boundary Element Methods in Mechanics*, vol. 3, *Computational Methods in Mechanics* (Edited by D. E. Beskos), pp. 285–331. Elsevier, Amsterdam.

Mukherjee, S. and Chandra, A. (1989). A boundary element formulation for design sensitivities in materially nonlinear problems. *Acta Mech.* **78**, 243–253.

Mukherjee, S. and Chandra, A. (1991). A boundary element formulation for design sensitivities in problems involving both geometric and material nonlinearities. *Math. Comput. Model.* **15**, 245–255.

Park, J. S. and Choi, K. K. (1990). Design sensitivity analysis of critical load factor for nonlinear structural systems. *Comput. Struct.* **36**, 823–838.

Rajiyah, H. and Mukherjee, S. (1987). Boundary element analysis of inelastic axisymmetric problems with large strains and rotations. *Int. J. Solids Structures* **23**, 1679–1698.

Rice, J. R. and Mukherjee, S. (1990). Design sensitivity coefficients for axisymmetric elasticity problems by boundary element methods. *Engng Anal. with Boundary Elements* **7**, 13–20.

Saigal, S., Borggaard, J. T. and Kane, J. H. (1989). Boundary element implicit differentiation equations for design sensitivities of axisymmetric structures. *Int. J. Solids Structures* **25**, 527–538.

Santos, J. L. T. and Choi, K. K. (1988). Sizing design sensitivity analysis of nonlinear structural systems; part II: numerical method. *Int. J. Num. Meth. Engng* **26**, 2097–2114.

Sladek, J. and Sladek, V. (1986). Computation of stresses by BEM in 2D elastostatics. *Acta Struct.* **31**, 523–531.

Tortorelli, D. A. (1988). Design sensitivity analysis for nonlinear dynamic thermoelastic systems. Ph.D. thesis, University of Illinois at Urbana-Champaign.

Tortorelli, D. A. (1990). Sensitivity analysis for nonlinear constrained elastostatic systems. In *Symposium on Design Sensitivity Analysis and Shape Optimization Using Numerical Methods* (Edited by S. Saigal and S. Mukherjee), pp. 115–126. ASME, New York.

Tsay, J. J. and Arora, J. S. (1990). Nonlinear structural design sensitivity analysis for path dependent problems, part 1: general theory. *Comput. Meth. Appl. Mech. Engng* **81**, 183–208.

Tsay, J. J. Cardoso, J. E. B. and Arora, J. S. (1990). Nonlinear structural design sensitivity analysis for path dependent problems, part 2: analytical examples. *Comput. Meth. Appl. Mech. Engng* **81**, 209–228.

Vanderplaats, G. N. (1983). *Numerical Optimization Techniques for Engineering Design*. McGraw-Hill, New York.

Wu, C. C. and Arora, J. S. (1987). Design sensitivity analysis and optimization of nonlinear structure response using incremental procedures. *AIAA Jl* **25**, 1118–1125.

Zabaras, N., Mukherjee, S. and Richmond, O. (1988). An analysis of inverse heat transfer problems with phase changes using an integral method. *ASME J. Heat Transfer* **110**, 554–561.

Zhang, Q. (1991). Shape design sensitivity analysis by the boundary element method. Ph.D. thesis, Cornell University, Ithaca, New York.

Zhang, Q. and Mukherjee, S. (1991a). Design sensitivity coefficients for linear elastic bodies with zones and corners by the derivative boundary element method. *Int. J. Solids Structures* **27**, 983–998.

Zhang, Q. and Mukherjee, S. (1991b). Second-order design sensitivity analysis for linear elastic problems by the derivative boundary element method. *Comput. Meth. Appl. Mech. Engng* **86**, 321–335.

Zhang, Q., Mukherjee, S. and Chandra, A. (1992). Design sensitivity coefficients for elasto-viscoplastic problems by boundary element method. *Int. J. Num. Meth. Engng* (in press).

APPENDIX

Equilibrium equations in the current configuration

The rate of equilibrium equation in terms of the Lagrange stress S in the reference (undeformed) configuration B^0 (in the absence of body forces) is

$$\dot{S}_{ij,i} = 0 \quad \text{so that} \quad 0 = \int_{B_0} \dot{S}_{ij,i}\, \mathrm{d}V = \int_{\partial B_0} N_m \dot{S}_{mj}\, \mathrm{d}S. \tag{A1, A2}$$

where $\mathrm{d}V$, $\mathrm{d}S$ and $\mathbf{N}$ are volume and surface elements and a unit normal to B_0 in the reference configuration, respectively.

Nanson's formula states that

$$\frac{n_i F_{im}}{J}\, \mathrm{d}s = N_m\, \mathrm{d}S. \tag{A3}$$

Hence, from eqns (A2) and (A3),

$$0 = \int_{\partial B} \frac{n_i F_{im}}{J} \dot{S}_{mj}\, \mathrm{d}s = \int_B \left(\frac{F_{im} \dot{S}_{mj}}{J} \right)_{,i} \mathrm{d}v.$$

Since this is true for arbitrary B, one gets the rate of equilibrium equation in the current configuration as

$$\left(\frac{F_{im} \dot{S}_{mj}}{J} \right)_{,i} = 0. \tag{A4}$$

It is interesting to note that the corresponding equation, without using rates (i.e. starting from $S_{ij,i} = 0$), gives the usual

$$\left(\frac{F_{im} S_{mj}}{J} \right)_{,i} = \sigma_{ij,i} = 0,$$

where σ is the Cauchy stress.

Lagrange traction rates

In the current configuration, the Lagrange traction rate is defined, eqn (17), as

$$\mathbf{t}^{(L)} = \frac{\mathbf{n} \cdot \mathbf{F} \cdot \dot{\mathbf{S}}}{J}.$$

It is easy to show, using Nanson's formula, that

$$\mathbf{t}^{(L)}\, \mathrm{d}s = \frac{\mathbf{n} \cdot \mathbf{F} \cdot \dot{\mathbf{S}}}{J} \mathrm{d}s = \mathbf{N} \cdot \dot{\mathbf{S}}\, \mathrm{d}S,$$

which is the basis of the definition of $\mathbf{t}^{(L)}$ [eqn (3.36) of Mukherjee and Chandra (1987)] in the updated Lagrangian formulation.

Formula for the current normal

A more convenient formula for the current normal is

$$\mathbf{n} = \mathbf{N} \cdot \mathbf{F}^{-1} / |\mathbf{N} \cdot \mathbf{F}^{-1}|,$$

where $|\ |$ denotes the absolute value of the vector.